Vibroacoustic analysis of composite thin fiberglass plate

Haydar Aygun, PhD

London South Bank University, School of the Built Environment and Architecture, 103 Borough Rd, London, SE1 0AA, UK. aygunh@lsbu.ac.uk and Haydar-aygun@hotmail.com

1. Introduction

The vibrations of the structures that are made of isotropic and homogeneous materials has been an important subject in the study of noise control, in the aeronautical industry, in the study of fluid-solid interactions and in construction industry for double leaf partitions as building structures. When a sound wave impinges on a structure, a part of acoustic energy is reflected back into source medium, a part is dissipated in the structure and the rest of acoustic energy is transmitted through the structure into the other medium. In building acoustics applications, the reflected acoustic energy builds up a reverberant sound field in the source room that in turn vibrates the walls. The vibrations in the common walls radiate sound directly into the receiver room. The vibrations in the other walls of the source room travel as structure-borne noise to the all walls of the receiving room and radiate sound into the receiver room.

Complex structures may be modelled as systems that are made of individual plate like elements. The theory of vibration of porous and non-porous structures is a well-known branch of engineering mechanics. Previous works on classical theory of the plate [1-7] has investigated vibration of isotropic and anisotropic plates for various boundary conditions. The vibration of porous plates can be described using two coupled equations [8], which are based on Biot's stress-strain relations [9, 10] and which introduce two types of compressional waves ('fast' and 'slow') and a shear wave. They assumed that the thickness of plate is smaller than the wavelength and that interaction can take place between the slow waves and the bending waves in the plate. They also ignored the amplitude of the fast wave. Galerkin's variational techniques were applied to porous plates [11-13], taking into account a classical set of trial functions obtained from the linear combination of trigonometric and hyperbolic functions for various boundary conditions. The effects of fluid loading on the vibration of rectangular porous plates and on their radiated sound power was investigated by including an extra term into the equations for the porous plate vibration, corresponding to the additional external force acting on the plate [14]. Previous study on low frequency vibration of porous plates [15] has demonstrated the existence of low frequency absorption coefficient resonance in configurations consisting of clamped poroelastic plates with an air cavity between the plates and a rigid termination. An analytical model that takes into account the effect of perforations and the effect of the flexural vibrations in the plates has been formulated and used to calculate the insertion loss in the absence, and in the presence of air flow [16, 17].

Recently, Aygun [18] has studied composite recycled glass bead panels in order to assess their suitability for civil engineering application, especially in noisy urban environments, either as structural panel components that also offer acoustic insulation or as dedicated noise barriers for outdoor applications. The aim of this paper is to investigate the vibrational and acoustical parameters of thin composite plates that are made of fiberglass, which are used for applications ranging from aerospace and automotive to construction industry. To author's best knowledge, vibroacoustical properties of composite plate have been reported in this paper for first time. The deflection of composite plate has been predicted at difference locations on the plate using the classical theory of the vibrating plate for simply supported and clamped boundary conditions. Computational simulations have been carried out to determine deformations of the plate in 3D for different frequency ranges for simply supported and clamped boundary conditions. Furthermore, the radiation impedance matrix has been predicted for simply supported boundary condition by using equations for eigenfunctions and Green's function without interpolation, convergence and without reducing the quadruple integral into a double integral.

2. Theory of plate vibration

When a flat plate is subjected to a transverse, time dependent force density $F(x, y, t)$, the transverse deflection of the plate is governed by the fourth order differential equation. The transverse vibration under free wave conditions stems entirely from inertial loading. A thin, baffled square plate of dimension *a* x *b* (along aces *x* and *y*, respectively) and uniform thickness *h* is considered in this study. The plate displacement induced by bending waves is in the direction of *z* axis and is function of time. The geometry of the plate is shown in Figure 1.

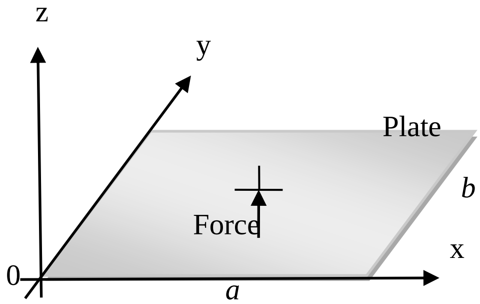

Figure 1: The geometry of a baffled plate.

The flexural wave equation for composite thin plate can be given by;

$$D\nabla^4 w_s + \rho_s h \ddot{w}_s = \begin{cases} 0, & free\ \ vibration \\ F(x,y), & forced\ \ vibration \end{cases} \tag{1- a, b}$$

where w_s is the transverse plate deflection, $\ddot{w}_s$ is the second order derivative of the plate deflection, $D = Eh^3/12(1-\nu^2)$ is the flexural rigidity, $\nabla^4 = \nabla^2(\nabla^2)$ and $\nabla^2 = \partial^2/\partial x^2 + \partial^2/\partial y^2$ in the system of coordinates (x, y) with x and y parallel to the plate sides of length a and b respectively, ρ_s is the mass density, E is the Young's modulus of the plate, and ν is the Poisson ratio of the plate.

The plate deflection w_s for harmonic wave motion is expressed in the form as shown below;

$$w_s(x,y) = \sum_{m=0}^{\infty}\sum_{n=0}^{\infty} A_{mn} X_m(x) Y_n(y) \tag{2}$$

where A_{mn} is the unknown coefficients to be determined, m, n = 0, 1, 2, 3 .....∞, and X_m and Y_n are the beam functions in x and y direction respectively.

The beam functions have been selected to satisfy different boundary conditions at the edges of the plate. An appropriate trigonometric function for vibrating beams has been used for X_m and Y_n different boundary conditions. For simply supported plates, the beam functions are

$X_m(x) = \sin(m\pi x/a)$, and $Y_n(y) = \sin(n\pi y/b)$ which should satisfy the equations of equilibrium. The boundary conditions for simply supported edges of the plate are $w = 0, \frac{\partial^2 w}{\partial x^2} = 0$, for $x = 0$ and $x = a$ and $w = 0, \frac{\partial^2 w}{\partial y^2} = 0$, for $y = 0$ and $y = b$. The shape of each mode of vibration of plate can be determined from Equation (2) by knowing the relative values of A_{mn} and the values of X_m and Y_n functions. In the static and dynamic analysis, the excitation function *F*(*x*, *y*) has been expanded into double infinite sine series of variables *x* and *y* for each value of the couple (m, n) by using the equation below;

$$F(x, y) = \sum_{m=0}^{\infty}\sum_{n=0}^{\infty} F_{mn} \sin(m\pi x/a) \sin(n\pi y/b) \tag{3}$$

where F_{mn} are the expansion coefficients.

By inserting (2) and (3) into (1), we can obtain that;

$$A_{mn} = F_{mn} / \left(D\nabla^4 - \omega^2 \rho_s h\right) \tag{4}$$

where ω is the angular frequency of the plate.

Trigonometric functions have been used to expand the plate deflection for clamped non-porous composite plate. These functions are called beam functions and are given by;

$$X_m(x) = B_{m1} \cosh(a_m x/a) + B_{m2} \cos(a_m x/a) + B_{m3} \sinh(a_m x/a) + B_{m4} \sin(a_m x/a) \tag{5-a}$$

$$Y_n(y) = C_{n1} \cosh(b_n y/b) + C_{n2} \cos(b_n y/b) + C_{n3} \sinh(b_n y/b) + C_{n4} \sin(b_n y/b) \tag{5-b}$$

where a_m and b_n are the frequency parameters corresponding to the m^{th} and n^{th} normal modes of characteristic equation.

The constants $C_{n1}, C_{n2}, C_{n3}, C_{n4}, B_{m1}, B_{m2}, B_{m3}, \text{ and } B_{m4}$ have been determined from the boundary conditions at four edges of the plate, and allow any condition involving simply supported, and clamped edges. A baffled square composite plate has been excited by a point force *F*(*x*, *y*, *t*) which is applied at x_0 = 0.25 m, and y_0 = 0.25 m from a corner of the plate. The responses have been calculated at the locations given by *x* = 0.25 m and *y* = 0.25 m and also at *x* = 0.15 m and *y* = 0.15 m respectively. The magnitude of the force used to vibrate the plate was 1 N. The vibration response of the plate has been calculated in the 0-1000 Hz frequency range. The properties of the plate used for numerical analysis are given in the Table 1.

Table 1: Properties of thin composite plate

Length (m)	Width (m)	Thickness (m)	Density (kg/m^3)	Young's Modulus (Pa)	Loss Factor	Poisson Ratio
0.50	0.50	0.0025	1600	7.489×10^9	0.03	0.2

The plate deflection have been predicted for values of *(m, n)* up to 30. The vibration responses of a simply supported and clamped composite plate plotted against frequency are shown in Figures 2. The responses observed are kind of exponentially decaying sinusoidal wave signal. The first and second resonance frequencies has been observed at 18 Hz and 91 Hz for simply supported plate respectively. In case of clamped plate, the first and second resonance frequencies has been observed at 33 Hz and 121 Hz respectively. It can be seen that clamping the plate at four edges delayed first resonance of the plate by 15 Hz and second resonance of the plate by 30 Hz while it reduces the amplitude of the plate deflection throughout the frequency range. The deflections of the composite plate has been also calculated at a point where x = 0.15 m and y = 0.15 m as shown in Figure 3. It shows that only amplitude of resonances changes at lower frequencies while at higher frequencies resonance and amplitude change.

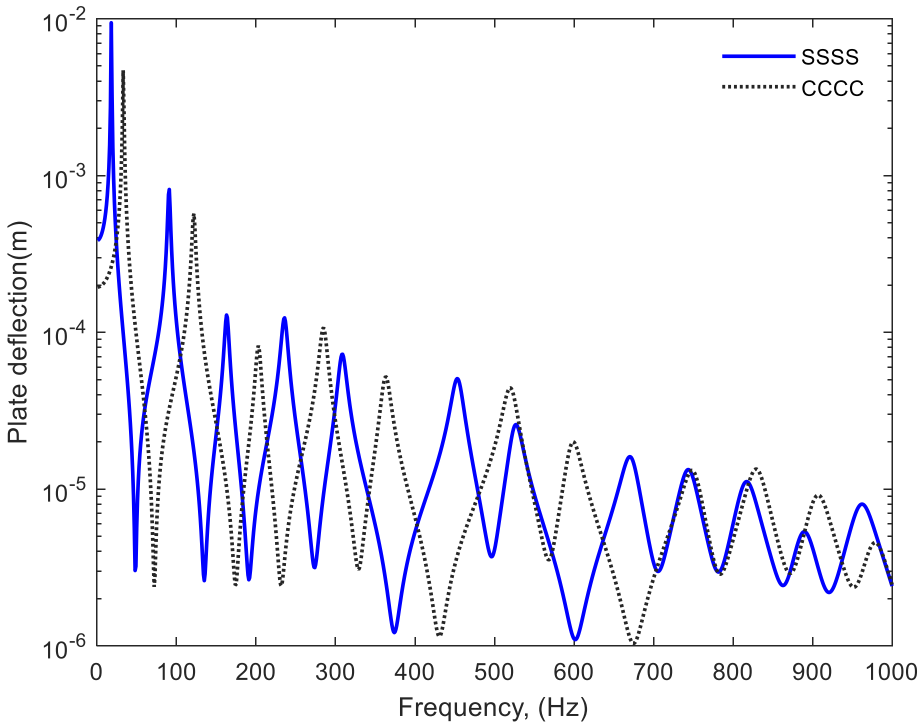

Figure 2: Deflection of simply supported and clamped fibreglass plate at x = 0.25m and y = 0.25m

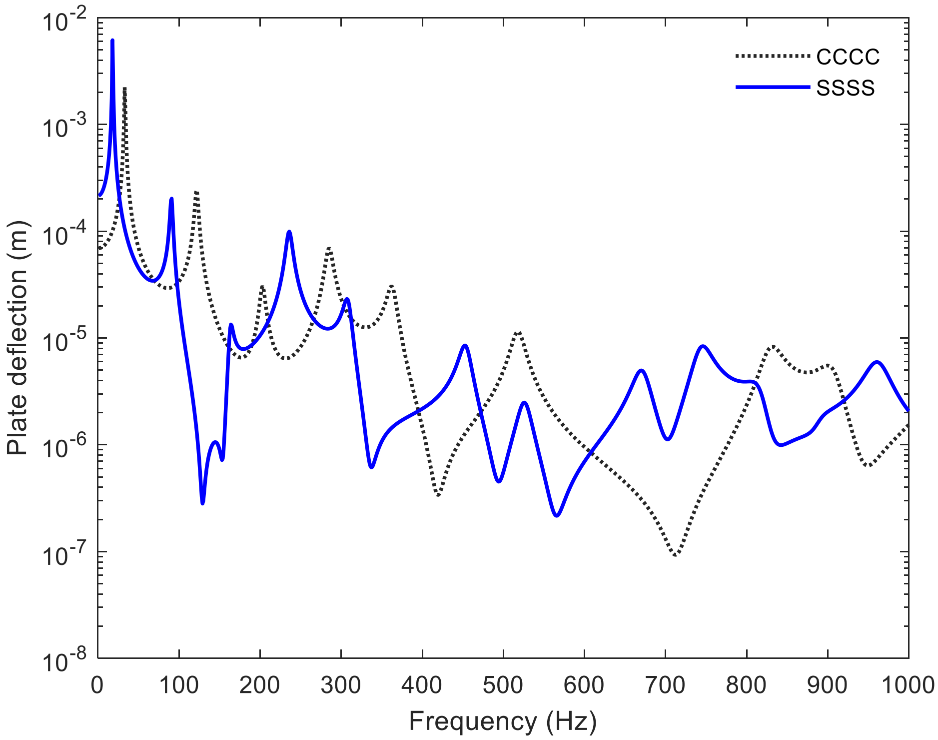

Figure 3: Deflection of simply supported and clamped fibreglass plate at x = 0.15 m and y = 0.15 m

3D deformations of thin composite plate for simply supported boundary condition are computed using a MATLAB code, at centre of the plate for 100 Hz, 500 Hz and 1 kHz, and their corresponding results are shown in Figures 4 a, b, and c respectively. 3D deformations for clamped composite plate are shown in Figure 4. Sixteen modes in each direction have been used to compute the 3D deformations of the composite plate. Vertical line at the centre of the plate shows the location where the force is applied to the plate. This clearly shows that different modal deformations at 100 Hz, 500 Hz and 1 kHz frequencies can be observed for different boundary conditions. 3D deformation in Figure 3a corresponds to first resonance frequency while the visualisation of the deformation in Figure 4a corresponds to first and second resonances. When the frequencies increase, the number of the plate resonances increase too.

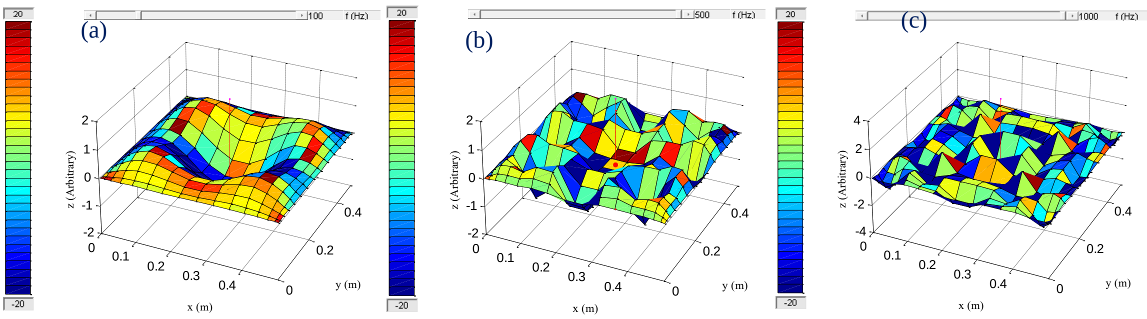

Figure 4: 3D deformation of fibreglass composite simply supported plate at a) 100 Hz, b) 500 Hz, and c) 1 kHz.

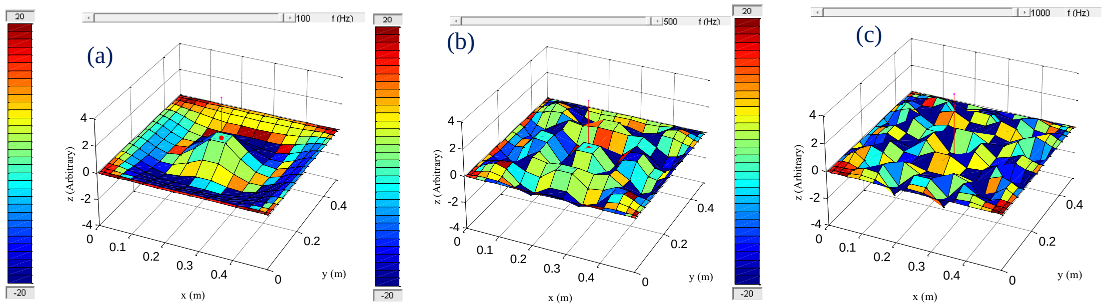

Figure 5: 3D deformation of fibreglass composite clamped plate at a) 100 Hz, b) 500 Hz, and c) 1 kHz respectively.

3. Radiation impedance matrix

The coefficients of the acoustic radiation impedance of a baffled plate are given by equation below:

$$Z_{mnpq} = j\rho\omega \iint_S \iint_S \psi_{mn}(x,y)\, G(x,y,z;x',y',0)\, \psi_{pq}(x',y')\, dS\, dS') \tag{6}$$

where Z_{mnpq} is known as the acoustic radiation impedance between the normal modes (*m, n*) and (*p, q*), $G(x,y,z;x',y',0)$ is the Green function defined, ρ is the fluid density, and $\psi_{pq}(x',y')$ is the eigenfunctions in the case of the simply supported boundary condition given by Equation (7);

$$\psi_{pq}(x',y') = \sin(\frac{p\pi x'}{a})\sin(\frac{q\pi y'}{b}) \tag{7}$$

The acoustic radiation impedance shows the influences of the sound pressure in the (*m, n*) mode on the plate system vibrating in the (*p, q*) mode. A Gaussian quadrature scheme with 16 terms of functions in each direction (*x, y*) has been used to compute the radiation impedance matrix. When the variables $x = x'$ and $y = y'$, for which $G(x,y,z;x',y',0)$ go to infinity, care has been taken to avoid singularity. The singularity at the origin has been avoided by taking G (0, 0) = 0. In this work the radiation impedance matrix has been calculated by using direct numerical integration of Equation (6) without interpolation, convergence and reducing the quadruple integral into a double integral. The direct and cross coupling terms of the radiation impedance matrix are normalized by the characteristic impedance ($\rho_0 c_0$), where ρ_0 is the air density and c_0 is the sound speed in the air.

The direct terms ($Z_{mnmn}/\rho_0 c_0$) of the radiation impedance matrix are shown in Figure 6. When higher values of (*m, n*) are used in the calculations, the radiation impedance matrix is equal to zero at low frequency. The cross coupling terms $Z_{mnpq}/\rho_0 c_0$ are shown in Figures 7. The values of *m, n, p,* and *q* vary between *0* and *N*. These figures show that the predicted radiation impedance matrix exhibits a smooth variation in terms of frequency. The real part of the radiation impedance matrix is the radiation resistance and expresses the radiation damping of the plate structure while the imaginary part of the radiation impedance matrix is the radiation reactance and expresses the added mass of gas on its structure.

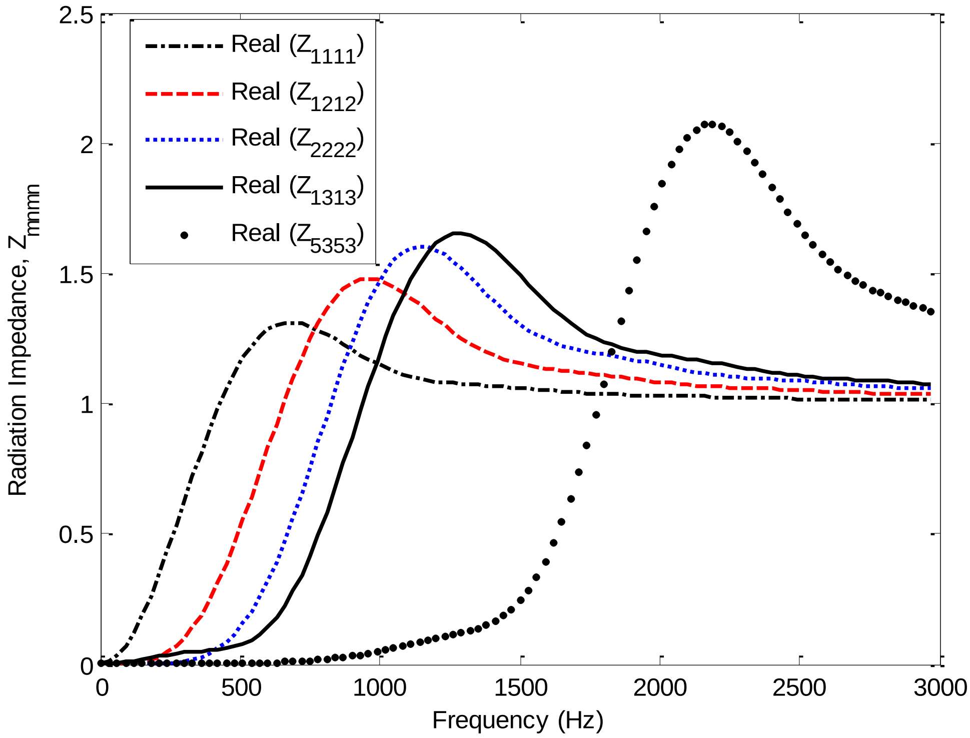

Figure 6: Radiation impedance matrix, direct terms.

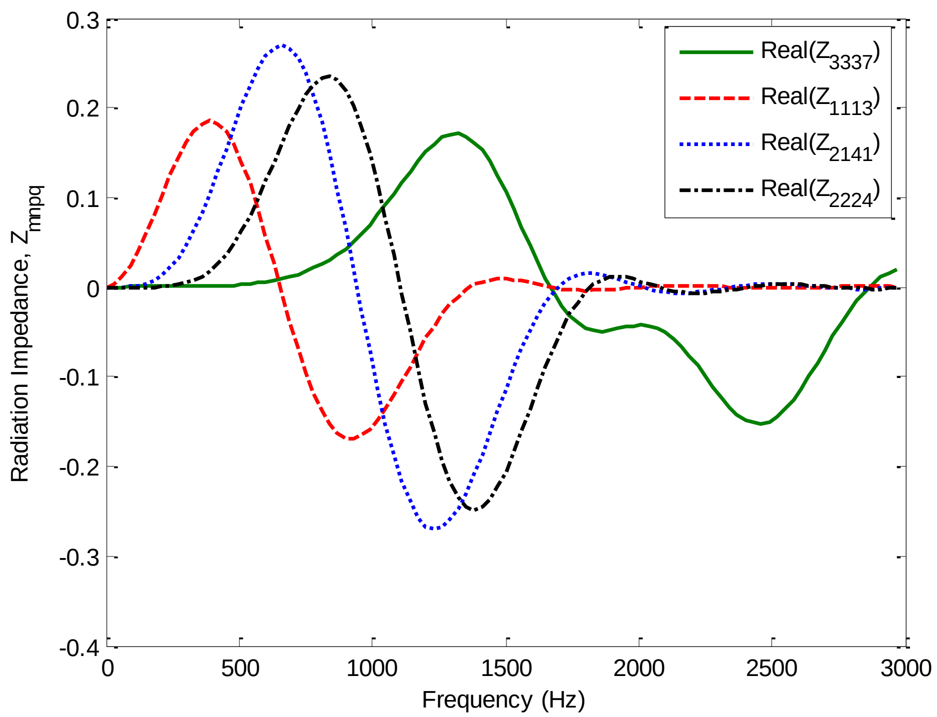

Figure 7: Cross coupling terms of the real part of the radiation impedance matrix

4. Conclusion

An investigation of the vibrational and acoustical parameters of thin composite plate that is made of fibreglass has been carried out. The deflection of the composite plate has been computed using the classical theory of the vibrating plate for simply supported and clamped boundary conditions at difference locations on the plate surface. Computational simulations have been carried out to determine deformations of the plate in 3D and their corresponding square velocities for different frequency ranges for simply supported and clamped boundary conditions. It has been shown that clamping the plate at four edges delayed first resonance of the plate by 15 Hz and second resonance of the plate by 30 Hz. The radiation impedance matrix has been calculated by using basic equation without interpolation, convergence and without reducing the quadruple integral into a double integral. The direct and cross coupling terms of the radiation impedance matrix have been normalized using characteristic impedance. The real part of the radiation impedance matrix is the radiation resistance and expresses the radiation damping of the plate structure. The imaginary part of the radiation impedance matrix that was not shown in the manuscript is the sound radiation reactance and expresses the added mass of gas on the plate structure.

5. Acknowledgement

This work was supported by London South Bank University Acoustic research Centre.

6. References

1) Waller, M. D.; "Vibrations of Free Square Plates: Part I Normal Vibrating Modes", Proceedings of the Physical Society of London, Vol. 51, Jun. 1939, pp. 831-844.
2) Waller, M. D.; "Vibrations of Free Square Plates: Part **11,** Compounded Nom1 Modes", Proceedings of the Physical Society of London, Vol. 52, Feb. 1940, pp. 452-455.
3) Warburton, G. B. "The Vibration of Rectangular Plates", Proceedings of the Institution of Mechanical Engineers, Vol. 168, No. 12, Jan-Dec 1954, pp. 371-384.
4) Hearmon, R. F. S. "The Fundamental Frequency of Vibration of Rectangular Wood and Plywood Plates", Proceedings of the Physical Society of London, Vol. 58, Jan. 1946, pp. 78-92.
5) Szilard, R.; “Theory and Analysis of Plates”. “Classical and Numerical Methods”. Prentice-Hall, Englewood, New Jersey, 1974.
6) Leissa, A. W.; “the free vibration of rectangular plates” J. Sound Vib. 1(3), 257-293(1973).
7) Young D., “Vibration of rectangular plates by the Ritz method,” Journal of Applied Mechanics 17, 448-453(1950).
8) Theodorakopoulos, D. D., and Beskos, D. E; “Flexural vibration of poroelastic plates,” Acta Mechanica, 103, 191-203 (1994).
9) Biot, M. A.; “Theory of elastic wave propagation in a fluid saturated porous solid. Part I-low frequency range,” J. Acoust. Soc. Am. 28,168-178(1956).
10) Biot, M. A.; “Theory of elastic wave propagation in a fluid saturated porous solid. Part 2-higher frequency range,” J. Acoust. Soc. Am. 28, 179-191(1956).
11) Leclaire, P., Cummings, A., and Horoshenkov, K. V.; “Transverse vibration of a thin rectangular porous plate saturated by a fluid,” J. Sound Vib. 247(1), 1-18 (2001).

12) Leclaire, P., Horoshenkov, K. V., Swift, M. J., and Hothersall, D. C.; "The vibration response of a clamped rectangular porous plate," J. Sound Vib. 217(1), 19- 31(2001).

13) Leclaire, P.; "Vibration of Porous Plates in Structural Acoustic Coupling Applications," 3rd European Congress on Acoustics. 16th –20th September 2002, Spain.

14) Aygun, H., and Attenborough, K.; "Predicted effects of fluid loading on the vibration of elastic porous plates". Acta Acoustica united with Acustica. 93(2) 2007: 284-289.

15) Aygun, H., and Attenborough, K.; "Sound absorption by clamped poroelastic plates," *J. Acoust. Soc. Am*. 124 (3) 2008, 1-7.

16) Aygun, H., and Attenborough, K.; "The insertion loss of perforated porous plates in a duct with and without mean air flow," *Applied Acoustics*, Vol.69 (2008), 506-513.

17) Aygun, H., and Attenborough, K: "Insertion loss of clamped perforated and non-perforated poroelastic plate silencers with flow," *Acta Acustica united with Acustica*, Vol. 94, Number 5, pp. 703-708(6), 2008.

18) Aygun, H. and McCann, F.; "Structural and acoustical performance of recycled glass bead panels". *Journal of construction and building materials*. Volume 258 (2020), 119581.